Experimental evidence of deviation from mirror reflection for acoustical shock waves

Régis Marchiano,* François Coulouvrat, and Sambandam Baskar
Institut Jean le Rond d'Alembert (UMR CNRS 7190), Université Pierre et Marie Curie–Paris 6, 4, place Jussieu 75252, Paris Cedex 05, France

Jean-Louis Thomas
Institut des NanoSciences de Paris (UMR CNRS 7588), Université Pierre et Marie Curie–Paris 6, 140, rue de Lourmel 75015, Paris, France

(Received 9 May 2007; revised manuscript received 30 August 2007; published 9 November 2007)

The reflection of plane waves on a perfectly reflecting surface is a well-known phenomenon in physics. This particular case of the famous Snell-Descartes laws, also called mirror reflection, is valid only for linear waves. For nonlinear shock waves, it is known that this law breaks for sufficiently grazing angles. This paper provides some experimental evidence of this phenomenon for amplitude more than 100 times as small as in previous measurements in air. This is achieved by means of ultrasonic periodic shock waves in water. For grazing angles (typically from 0° to 7°) three different patterns exhibiting strong differences with the mirror law can be observed. The first one is the nonlinear regular reflection for which the incident shock and the reflected one merge on the rigid surface but the incident and reflected angles are different. The second pattern looks similar to the Mach reflection in aerodynamics. In this case, three shocks are present: the incident and reflected shocks merge just above the rigid surface into a third one connected to the rigid surface. In the third pattern, only the incident shock is visible. These experimental results are successfully compared with a theory through accurate numerical simulations.

DOI: 10.1103/PhysRevE.76.056602 PACS number(s): 43.25.+y

Mirror reflection is a very fundamental law in physics, from particles (such as billiard balls) to waves (light, sound, or tide). It can be viewed as a particular case of the Snell-Descartes laws. Nevertheless, deviations from mirror reflection exist. In aerodynamics, Mach [1] was the first scientist to observe experimentally a discrepancy for strong nonlinear shocks. Reflection of strong shocks can be divided into regular and Mach reflections [2]. Regular reflection is a generalization of mirror reflection where the incident and reflected shocks meet on the reflecting surface, but the reflected angle is different from the incident one. On the contrary, for the Mach reflection, the incident and reflected shocks merge above the surface into a third one, called Mach stem or Mach shock, connected to the surface. For a Mach reflection, the reflection pattern looks similar to a "Y" with three straight shocks (without curvature). The point where the three shocks meet is called the triple point. This behavior has been well known in aerodynamics since the experimental works of Mach and theoretical studies of von Neumann [3]. Regular reflection is described by the two-shock theory while Mach reflection is described by the three-shock theory. These theories are well adapted for strong shocks, but for shock Mach numbers less than 1.05, the three-shock theory fails to predict the Mach reflection [4]. Nevertheless, there exist numerical and experimental studies exhibiting this phenomenon [5,6]. The main difference on the reflection pattern is that the stem has a curvature. This regime is called von Neumann reflection and the discrepancy between theoretical results and experimental/numerical ones is known as the von Neumann paradox. Numerous studies are devoted to solving this point (see the review of Ben Dor [2]). The goal of this paper is not to explain this paradox but to demonstrate experimentally and numerically that it occurs in nonlinear acoustics. Indeed, the framework of the existing studies is mainly aerodynamics for which the amplitude of the incident shock is always high. For weak shocks, this paradox has been shown, theoretically and numerically, to occur whatever the amplitude, provided the angle is grazing enough [7]. But, in all the previous studies the shocks are step shocks whereas in the experiments presented here shocks are periodic sawtooth waves. This difference is crucial since periodicity and shape of shocks are expected to modify the regime of reflection [8]. In acoustics, extremely weak shock waves do exist, resulting from the linear dependence of the sound speed in the instantaneous pressure amplitude p, according to the law

$$c = c_0 + \frac{\beta p}{\rho_0 c_0}, \tag{1}$$

where ρ_0 and β are, respectively, the ambient density and the nonlinear parameter of the medium associated to quadratic nonlinearities. Equation (1) is valid for any classical fluid such as air or water [9,10]. This formula remains valid for the shock speed itself by replacing p by the mean value of the pressure just before and after the shock. Acoustical shock waves can be encountered in many situations: thunder, sonic boom, or ultrasonic devices used in therapy. For each case the temporal shape of the pressure is never a step shock but is either an N wave or a periodic sawtooth wave. In this last case, the shock speed is exactly the linear sound speed c_0 because of the antisymmetry of the waveform. The aim of this paper is to demonstrate experimentally that, for grazing incidences, reflection of acoustical shock waves strongly dif-

*marchi@lmm.jussieu.fr

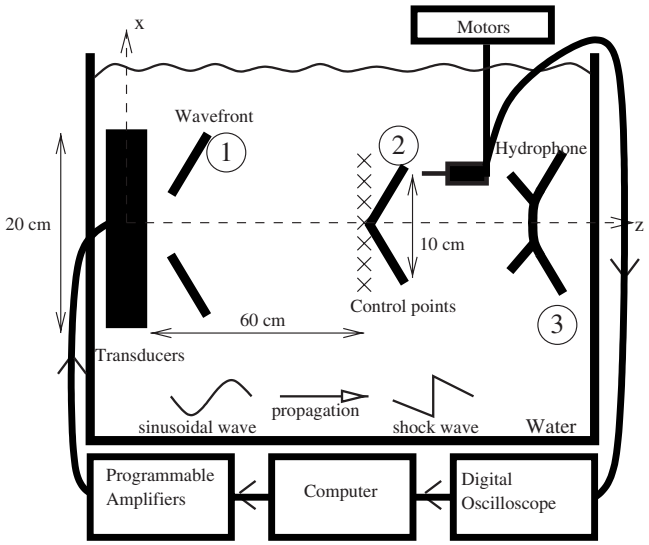

FIG. 1. Experimental setup. The evolution of the wavefront is sketched as follows: (1) two symmetrical plane waves are emitted from the transducers, (2) they meet 60 cm away from the array to give birth to a wavefield satisfying the reflection condition [see Eq. (2)], (3) they interact nonlinearly giving birth to a nonlinear reflection pattern.

fers from the classical mirror theory even if parameter $M-1$ (M is the Mach number defined as the ratio between the shock velocity relative to the media ahead immediately upstream of the shock and the speed of sound in the media immediately upstream of the shock [11]) is here only 2.3×10^{-4}, two orders of magnitude smaller than previous experiments in air (not less than 0.04 [6,12])

To observe experimentally the reflection of acoustical shock waves on a perfectly rigid surface, ultrasonic shock waves in water are used. The experimental setup (Fig. 1) is composed of an array of 256 piezoelectrical transducers (central frequency $\omega_0/2\pi=1$ MHz, total size 80 mm $\times$191 mm) radiating a plane wave with an amplitude up to $p_0=0.5$ MPa. For this amplitude and fundamental frequency, the distance of shock formation for a plane wave $L=\frac{\rho_0 c_0^3}{\beta\omega_0 p_0}$ is about 30 cm. Due to the limited bandwidth of the transducers, only tone bursts can be emitted. Shock waves are produced through the waveform steepening induced by nonlinear propagation. According to classical theory of nonlinear acoustics, for a plane wave the shocks appear beyond the shock formation distance $z=L$. This enables us to obtain well-formed shocks within the measurement area between 60 cm and 1 m away from the transducers. A broadband membrane hydrophone is used to record the pressure field. This hydrophone is calibrated from 1 to 50 MHz. It is very well adapted to measure shock waves. Moreover, the size of the probe (0.2 mm large) allows us to measure the quick spatial variations of the pressure field (the Mach stem measures about 1 mm—see experimental results). It can be moved in the three directions of space thanks to three step-by-step motors. The signal sent by each transducer is determined by the inverse filter technique.

The inverse filter technique is a linear technique of complex wavefield synthesis [13]. It is based on the knowledge of the propagation operator between a set of acoustical sources (the transducers) and a set of control points. Here, the acoustical sources are the different transducers of the array and the set of control points is chosen as a line of 67 points evenly spaced along 10 cm in the transverse x direction, located 60 cm away from the transducers ($\approx 2L$). First, the propagation operator is experimentally recorded and then numerically inverted. This inversion is finally used to compute the signal to be sent by each transducer in order to synthesize the desired pattern. This is technically possible thanks to programmable amplifiers driving individual transducers. However, in water, a perfectly rigid surface cannot be realized because its density is comparable to any other metal (even the gold density is only 19.6 times the water one). To overcome this impossibility to have a perfectly rigid surface, we rely on the mathematical equivalence between rigid reflection and symmetry conditions, both expressed by

$$\left.\frac{\partial p}{\partial x}\right|_{x=0} = 0. \tag{2}$$

Indeed, this equivalence [Eq. (2)] is fundamental for perfect reflection, for which any physical source has its virtual counterpart image, hence the name of mirror reflection taken from optics. In our experiment, that symmetry condition is perfectly achievable through the inverse filter technique. Indeed, the pattern along the control line ($x=0$) is imposed to be two half-plane waves, symmetrical about the propagation axis Oz (Fig. 1) with a prescribed grazing angle θ (defined as the angle between the wavefront and the normal to the reflecting surface). Thus, the distance where the pattern is imposed is thus the beginning of the reflection. Indeed, before this distance, the field is more or less two plane waves totally disconnected as sketched in Fig. 1. However, as the inverse filter technique is linear, at this stage it is only possible to deal with the mirror reflection of linear acoustical waves (without shock waves). Experimentally, we check that the linear field satisfies the linear Snell-Descartes theory for any incident angle (not shown here). Then, the same signals are sent but with a high amplitude, so that nonlinear effects take place during the propagation according to Eq. (1) and shock waves appear. As nonlinear effects are locally small (a relative perturbation of less than 10^{-3}), the main features of the linear pattern, and especially the symmetry condition and the fixed incidence angle, remain almost up to the control line where the two half-plane waves begin to interact. This enables us to perform an experimental measurement of nonlinear acoustical shock wave grazing reflection. Note that measurements of nonlinear acoustical wave focusing present many analogies with our experiment [7]. Indeed, focusing can be viewed as a reflection across an axis of symmetry. Moreover earlier experiments have shown the existence of Mach reflection for focusing [12]. Nevertheless, these studies deal with either strong shock or step shocks since amplitude and waveform are crucial parameters used to investigate accurately this phenomenon. The modeling used in this paper, Refs. [7,14,15,8], relies on the paraxial approximation of the

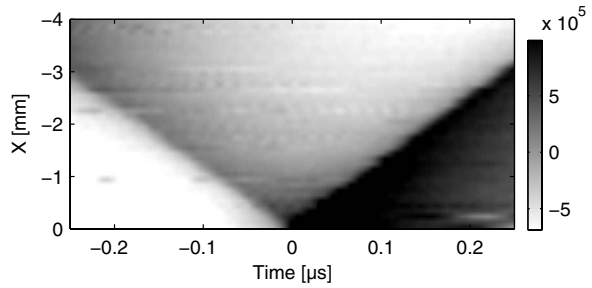

FIG. 2. Pressure field (in Pa) for $\theta=7°$: Experimental result.

nonlinear wave equation, which is known as the Khokhlov-Zabolotskaya (KZ) equation [16]

$$\frac{\partial^2 P}{\partial Z \partial \tau} = \frac{\partial^2 P}{\partial X^2} + \frac{\partial P^2}{\partial \tau^2}. \tag{3}$$

The dimensionless variables are defined as follows: $P = p/p_0$ for the pressure, $Z = z/L$ for the longitudinal variable, $X = x\sqrt{\omega_0^3 L/2c_0^3}$ for the transverse variable, and $\tau = \omega_0(t - z/c_0)$ for the retarded time. Equation (3) takes into account the interaction between transverse diffraction and nonlinear effects (the two terms on the right-hand side) as the wave propagates (the left-hand side). This equation is valid as long as propagation remains located along the propagation axis (typically it is valid up to 15°, while here grazing angles will not be larger than 7°). Far away from the symmetry axis, the incident shock wave is assumed to be perfectly plane and therefore satisfies Eq. (3) without the diffraction term. It can be written [8]

$$P(X,Z,\tau) = G(Z)F(\tau + aX + a^2 Z), \tag{4}$$

where F is the waveform of the incoming signal and G its amplitude (depending on F). The phase of the signal $\tau + aX + a^2 Z$ is the one of a plane wave with grazing angle, which introduces the dimensionless critical parameter a:

$$a = \frac{\sin(\theta)\sqrt{\rho_0 c_0^2}}{\sqrt{2\beta p_0}}. \tag{5}$$

It compares the effects of diffraction associated to the grazing angle, to nonlinearities [8]. On the rigid surface, the symmetry/reflection condition is given by Eq. (2). To numerically solve the KZ equation and its associated boundary equations, a modified version [8] of an existing algorithm [17,18] has been used. The waveform F of the incoming signal is extracted from the experimental data on the control line (at this distance there is almost no reflection yet). This experimental signal is used as an input to (1) calculate the a parameter, (2) compute the nonlinear amplitude evolution $G(Z)$, and finally (3) solve the KZ equation for comparisons with measurements.

Figures 2–5 show the spatiotemporal pressure field. The x axis is the delayed time τ and the y axis is the distance from the symmetry axis ($y=0$ is the location of the symmetry axis or equivalently the location of the reflector). For each figure, the color of a pixel represents the pressure amplitude of the field at point x and time τ and the color bar indicates the pressure levels in pascals. In order to visualize the local phenomenon of nonlinear reflection better, the figures are displayed with a shorter temporal window than the period of the signal. Thus, the periodicity of the acoustical signals is not visible in the figures, but this is just an artifact of visualization since the signals are periodic. The measurements are performed perpendicularly to the symmetry axis along a 2 cm segment located 9 cm behind the control line, where the reflection begins. The spatial sampling is 0.2 mm (which is the size of the active part of the hydrophone). The temporal sampling is 1 GHz. The figures are displayed, respectively, for four different incidence angles, namely, $\theta=1°$, 3°, 5°, and 7°. The experimental results (top of each figure) are systematically compared (except for the case $\theta=7°$) to the

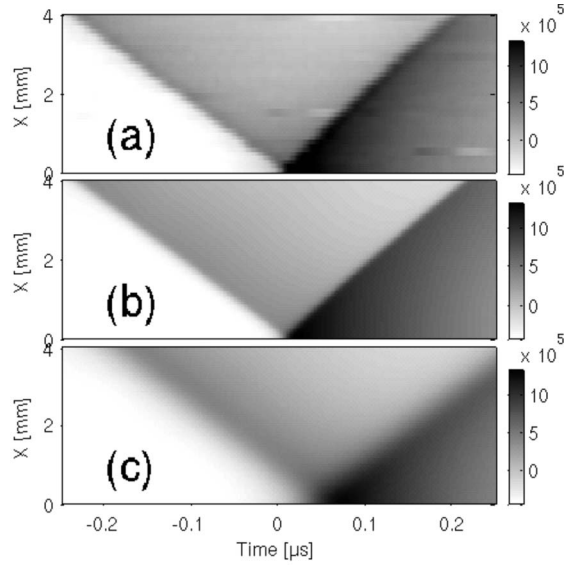

FIG. 3. Pressure field (in Pa) for $\theta=5°$: (a) Experimental result, (b) nonlinear simulation, (c) linear simulation.

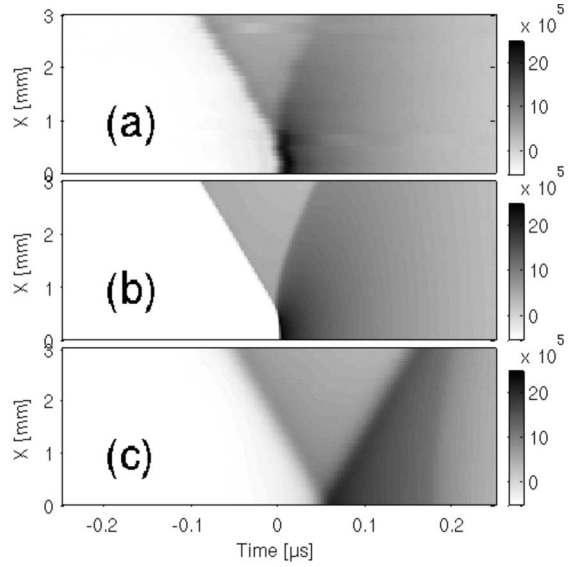

FIG. 4. Pressure field (in Pa) for $\theta=3°$: (a) Experimental result, (b) nonlinear simulation, (c) linear simulation.

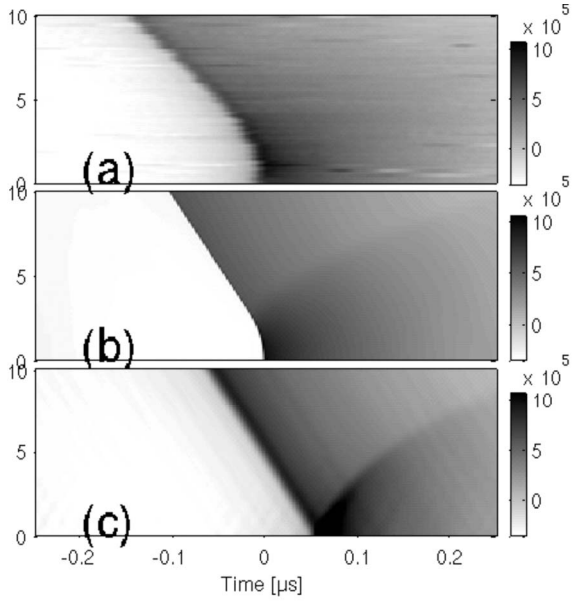

FIG. 5. Pressure field (in Pa) for $\theta=1°$: (a) Experimental result, (b) nonlinear simulation, (c) linear simulation.

numerical simulation of Eq. (3) (middle figure). Also, to better visualize the deviation from mirror reflection, a numerical simulation in the linear regime is also included (bottom figure), with the nonlinear term of Eq. (3) omitted.

For the angle $\theta=7°$ (Fig. 2), though we obviously have an incident shock wave whose amplitude is about 0.5 MPa (visible as the straight line separating the white and the gray areas), we nevertheless observe a classical mirror reflection: the incident angle is equal to the reflected one (also a shock wave of about the same amplitude, separating the gray and black areas).

For the angle $\theta=5°$ (Fig. 3), the reflection is still regular with two shocks connected on the symmetry axis $x=0$. The value of the parameter a [see Eq. (5)] is 1.81. This value is in agreement with theoretical results which predict that regular reflection exists while a is greater than $\sqrt{2}$. However, the nonlinear effects [Figs. 3(a) and 3(b)] are now clearly visible as the reflected shock angle $\theta=c_0\Delta t/\Delta x\approx 4°$ is smaller than the incident one. This value is in good agreement with von Neumann two-shock theory. The deviation from mirror reflection is also exemplified by comparisons with linear simulation [Fig. 3(c)]. In that last picture the contact point arrives later because nonlinear effects that accelerate shock propagation according to Eq. (1) do not occur.

The situation turns out dramatically different for the smaller angle $\theta=3°$ [Figs. 4(a) and 4(b)]. The regular two-shock pattern is completely broken. The value of a is 0.91. This value is in agreement with theoretical predictions stating that regular reflection cannot exist for values of a less than $\sqrt{2}$. This behavior is analogous to the von Neumann reflection phenomenon known in aerodynamics for moderate step shocks. The incident and reflected shocks do not merge on the rigid/symmetry line. Instead of the classical two-shock pattern, the experimental observation shows a situation with three different shocks. The Mach stem is not a straight line but has a smooth and regular slope with maximum curvature near the triple point and, consequently, the contact point of the Mach stem arrives sooner (about 0.1 μs). There is an excellent agreement between the experimental results and the nonlinear simulation. The size of the Mach stem (about 0.75 mm) and the curvature of the Mach and reflected shocks are comparable with the experimental ones. Also, the pressure amplitude in all points of the field is well reproduced with the same local amplification right behind the Mach stem (with a factor 2.5 versus 2 for the linear case). That amplification implies the Mach stem propagates faster and hence creates a curvature. At the opposite, the linear simulation [Fig. 4(c)] totally misses all the above features. This undoubtedly demonstrates that diffraction cannot be the only physical mechanism responsible for this special reflection pattern, which is intrinsically coupled to nonlinearities. Note that, contrary to the usual nonlinear propagation, this is an extremely local phenomenon (subwavelength compared to the fundamental wavelength, here 1.5 mm).

If the grazing angle is zero, then there is no reflection at all; the incident wave remains unaffected. Therefore, another transition has necessarily to occur to match the von Neumann reflection described above (with three shocks) to the perfectly grazing case with no reflection at all (with only one shock). Indeed, for extremely small deviation from perfect grazing the perturbation of the incident wave has to be extremely small also and therefore cannot be a shock wave. So, for small values of the grazing angle, we expect a pattern with one shock. This is exactly what is observed experimentally for $\theta=1°$ [Figs. 5(a) and 5(b)]. This regime has never been observed to our knowledge. It is different from the von Neumann reflection since no reflected shock is visible. It is similar to a weak von Neumann reflection. The value of $a=0.36$ supports again the theory [8] which predicts this new regime for $a<0.4$. The effects on the incident shock for the von Neumann reflection and the weak von Neumann reflection are similar. They are essentially characterized by the curvature near the reflector. The essential difference lies in the reflected shock whose amplitude decreases progressively with the grazing angle up to disappearance for the weak von Neumann case. Even if this regime corresponds to an extremely weak reflection, it is nevertheless very different from the linear reflection [Fig. 5(c)]. This may sound paradoxical but it is not, as pointed out by von Neumann himself in his seminal paper [3]. Indeed, he outlined that the linear mirror reflection is singular in the sense that it does not allow a continuous transition between reflection regime and perfect grazing (for instance, the pressure at the surface will double for any grazing angle except the zero value). The transition from grazing angle to zero angle follows this scheme: first the classical mirror reflection (two shocks, observed here for $\theta=7°$) which can be analyzed by linear theory even for nonlinear shock waves, second the regular reflection (two shocks, observed here for $\theta=5°$), third the von Neumann reflection (three shocks, observed here for $\theta=3°$), and fourthly the weak von Neumann reflection (one shock, observed here for $\theta=1°$). These last three patterns are observed for acoustical and weak von Neumann waves. To our point of view, these observations open interesting outlooks to better understand the acoustical paradox of von Neumann.

[1] E. Mach, Sitzungsbr. Akad. Wiss. Wien **78**, 819 (1878).
[2] G. Ben-Dor, *Shock Wave Reflection Phenomena* (Springer Verlag, New York, 1992).
[3] J. von Neumann, in *John von Neumann Collected Works*, edited by A. H. Taub (Pergamon, New York, 1943), Vol. 6, pp. 238–299.
[4] P. Colella and L. F. Henderson, J. Fluid Mech. **213**, 71 (1990).
[5] A. M. Tesdall and J. K. Hunter, SIAM J. Appl. Math. **63**, 42 (2002).
[6] B. W. Skews and J. T. Ashworth, J. Fluid Mech. **542**, 105 (2005).
[7] E. Tabak and R. R. Rosales, Phys. Fluids **6**, 1874 (1994).
[8] S. Baskar, F. Coulouvrat, and R. Marchiano, J. Fluid Mech. **575**, 27 (2007).
[9] O. V. Rudenko and S. I. Soluyan, *Theoretical Foundations of Nonlinear Acoustics* (Consultant Bureau, New York, 1977).
[10] M. F. Hamilton and D. T. Blackstock, *Nonlinear Acoustics* (Academic Press, San Diego, 1998).
[11] G. B. Whitham, *Linear and Nonlinear Waves* (Wiley, New York, 1974).
[12] B. Sturtevant and V. Kulkarny, J. Fluid Mech. **73**, 651 (1976).
[13] R. Marchiano, J.-L. Thomas, and F. Coulouvrat, Phys. Rev. Lett. **91**, 184301 (2003).
[14] J. K. Hunter, in *Multidimensional Hyperbolic Problems and Computations*, edited by A. J. Majda and J. Glimm, Vol. 29 of IMA Volumes in Mathematics and Its Applications (Springer, Berlin, 1991), pp. 179–197.
[15] J. K. Hunter and M. Brio, J. Fluid Mech. **410**, 235 (2000).
[16] E. A. Zabolotskaya and R. V. Khokhlov, Sov. Phys. Acoust. **15**, 35 (1969).
[17] R. Marchiano, F. Coulouvrat, and J. L. Thomas, J. Acoust. Soc. Am. **117**, 566 (2005).
[18] F. Coulouvrat and R. Marchiano, J. Acoust. Soc. Am. **114**, 1749 (2003).